

## MECHANICAL COMPENSATION OF POWER LOSS IN THE ENDURANCE TESTS ON ROTARY AND LINEAR POSITIVE DISPLACEMENT MACHINES

Teodor Costinel POPESCU<sup>1</sup>, Radu Iulian RĂDOI<sup>1</sup>, Mihai-Alexandru HRISTEA<sup>1</sup>

<sup>1</sup>)INOE 2000-IHP Bucharest; popescu.ihp@fluidas.ro

**Abstract:** Through experimental tests and numerical simulations the authors of this paper demonstrate a method of reducing energy consumption on the endurance stands of rotary and linear positive displacement machines. The method is based on mechanical compensation of power losses, achieved by coupling the drive shafts of two positive displacement machines, a pump and a rotary motor, with pump capacity greater than motor capacity and equal rotary speeds. The method can be applied in the simultaneous endurance tests on the two rotary positive displacement machines, and by extension, on the endurance test stands designed for hydraulic cylinders.

**Keywords:** Mechanical compensation of power loss, endurance, rotary and linear positive displacement machines

### 1. Introduction

Mechanical compensation of power losses [1] can be done on the power recirculation stand in the Figure 1, used for endurance tests on rotary positive displacement machines, and also on the power recirculation stand in the Figure 2, used for endurance tests on linear positive displacement machines.

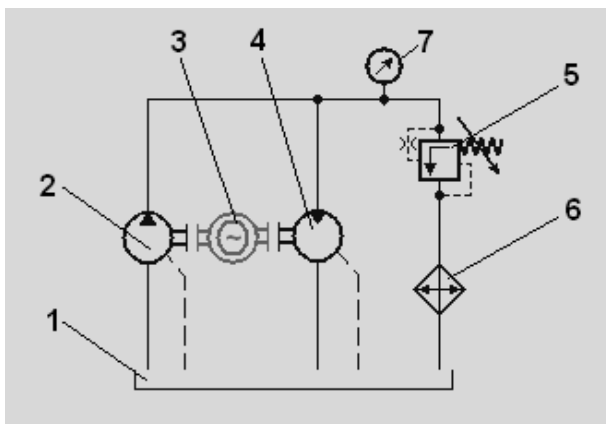


**Fig. 1.** Power recirculation at endurance tests on rotary positive displacement machines:  
 1=tank; 2=fixed pump; 3= two-axis electromotor;  
 4=hydraulic motor; 5= pressure control valve;  
 6= return filter; 7=pressure gauge

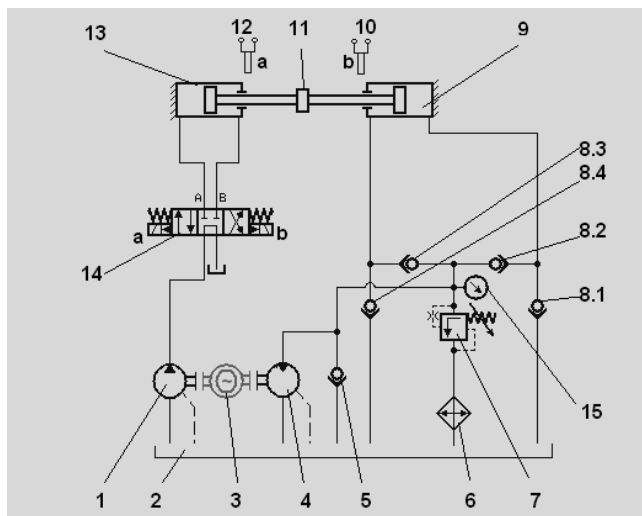


**Fig. 2.** Power recirculation at endurance tests on linear positive displacement machines

The tank, pump, electromotor, hydraulic motor, control valve, filter and pressure gauge which make up the stand in the Figure 1 can also be found in the structure of the stand in the Figure 2. For both stands the capacity of the pump is higher than the capacity of the hydraulic motor, and the rotary speeds are equal.

In addition, the stand in the Figure 1 also contains the following parts [2]: 5= non-return valve for supplying the hydraulic motor in the "non-actuated" position of the hydraulic directional valve with electrical control 14; 8.1, 8.2, 8.3, 8.4= non-return valves for supplying / discharging the chambers of the load cylinder 9; 10, 12=stroke limiters; 11=coupling; 13=test cylinder.

For the stand in the Figure 1 a demonstrative experimental module has been developed in order to promote the method of compensation for power losses at the stands for endurance tests, with low energy consumption, of rotary and linear positive displacement machines.

## 2. Experimental determinations of recovered energy in endurance tests on positive displacement machines

### 2.1. The demonstrative experimental module

The hydraulic basic diagram of a small demonstrative stand is shown in the Figure 3 and it comprises: a fixed positive displacement pump with a capacity of  $6 \text{ cm}^3/\text{rev}$  (2) and a fixed positive displacement motor (3), with a capacity of  $4 \text{ cm}^3/\text{rev}$ , both coupled to an electric motor (1), of 0.37 kW, with a constant rotary speed of 1375 rev/min; a pressure control valve (4); a 4/3 hydraulic directional valve, with electric control (5), a pressure gauge (6) and an oil tank (7).

Physical development of the experimental demonstrative module, which in order to couple the electromotor to the pump and hydraulic motor axes uses a gear transmission, with 1:1 transmission ratio, is shown in the Figure 4.

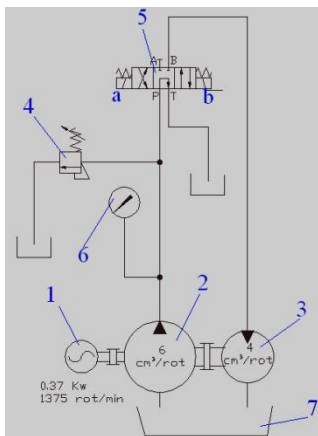


**Fig. 3.** Hydraulic diagram of the experimental demonstrative module

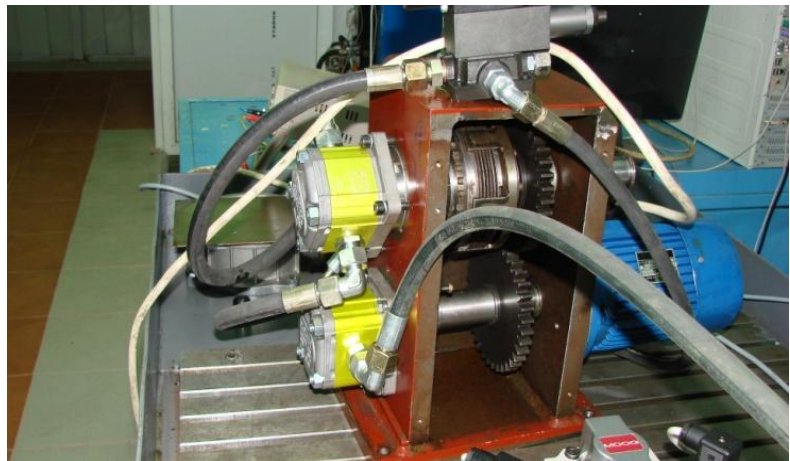


**Fig. 4.** Physical development of the experimental demonstrative module

In order to test the energy recovery system only the extreme switch positions of the sliding valve of the 4/3 hydraulic directional control valve are used (excluding the center position).

When the electromagnet "b" of the directional control valve is actuated, there is achieved the distribution "P" to "A" (a plug was fitted on "A") and "B" to "T", the entire flow of the pump is discharged through the valve to the oil tank, the hydraulic motor feeds from the tank, being driven at the same time with the pump by the electric motor, but it does not generate a mechanical torque and does not "help" the electric motor which drives the two positive displacement machines.

When the electromagnet "a" of the directional control valve is actuated, there is achieved the distribution "P" to "B" and "A" to "T", (the plug remains fitted on "A"). The discharged flow of the pump is divided into: 5.5l/min, entering the hydraulic motor, and 2.75l/min, conveyed through the pressure control valve. The hydraulic motor is supplied by the pump and it is driven, simultaneously with the pump, by the electromotor. In this situation the hydraulic motor contributes to the production of part of the mechanical torque required to actuate the positive displacement pump.

### 2.2. Experimental results

**By using the test stand shown in the Figure 4 there have been measured:** pump discharge pressure -  $p$  (bar); single phase electric current absorbed by the motor -  $I$  (A) and electric motor speed -  $n_{me}=n_p=n$  (rev/min).

To plot the experimental characteristics there have been calculated: hydraulic power generated by the pump -  $P_h$  (W); power absorbed by the electric motor -  $P_a$  (W); power output generated by the electric motor -  $P_u$  (W) and mechanical power generated by the hydraulic motor -  $P_{mh}$  (W).

The following equations have been used:

$$P_h = \frac{V_p \cdot n_p \cdot p}{\eta_p \cdot 612} \tag{1}$$

where:  $P_h$  – hydraulic power (W);  $V_p$  - pump capacity ( $cm^3/rev$ );  $n_p$  – pump speed, which is equal to hydraulic motor speed  $n_{mh}$  ( $rev/min$ );  $p$  – pump discharge pressure (bar);  $\eta_p$  – total pump efficiency (-); 612 – dimensionless factor (-).

$$P_a = 3U \cdot I \cdot \cos \varphi \tag{2}$$

where:  $P_a$  – power absorbed by the electric motor (W);  $U$  – phase voltage (V);  $I$  – electric current intensity (A);  $\cos \varphi = 0.71$ .

$$P_u = P_a \cdot \eta_{me} \tag{3}$$

where:  $P_u$  – power output generated by the electric motor (W);  $\eta_{me}$  – electric motor efficiency (-).

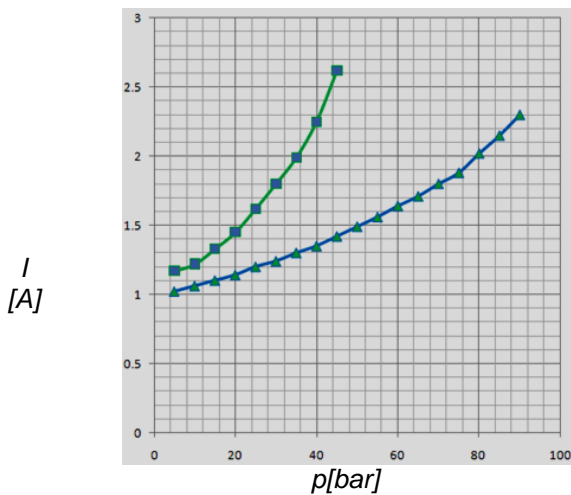


Fig. 5. The  $I=f(p)$  characteristic

Series 1: P to A; Series 2: P to B

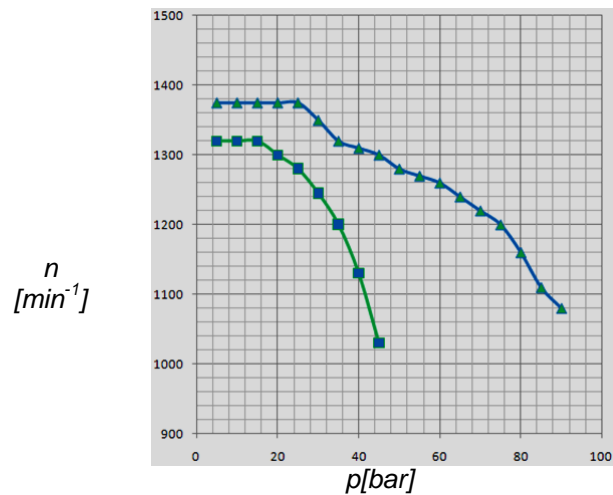


Fig. 6. The  $n=f(p)$  characteristic

Series 1: P to A; Series 2: P to B

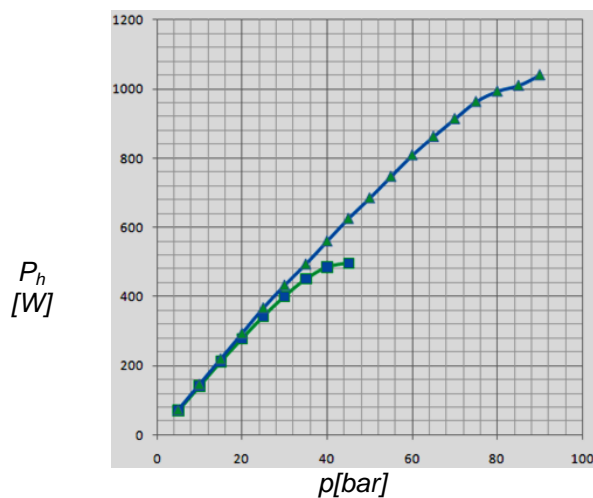


Fig. 7. The  $P_h=f(p)$  characteristic

Series 1: P to A; Series 2: P to B

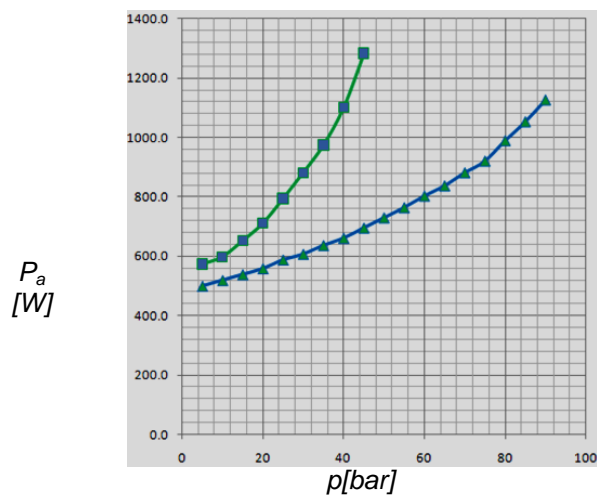


Fig. 8. The  $P_a=f(p)$  characteristic

Series 1: P to A; Series 2: P to B

$$P_{mh} = \frac{V_{mh} \cdot n_{mh} \cdot p \cdot \eta_{mh}}{612} \quad (4)$$

where:  $P_h$  – hydraulic power (W);  $V_{mh}$  - hydraulic motor capacity ( $cm^3/rev$ );  $n_{mh}$  – hydraulic motor speed ( $rev/min$ );  $p$  – hydraulic motor intake pressure (bar);  $\eta_{mh}$  – total hydraulic motor efficiency (-); 612 – dimensionless factor (-).

The figures 5...8 depict four characteristics determined experimentally, namely: variation of the current absorbed by the electric motor  $I$  [A] (Fig. 5), variation of electric motor speed  $n$  [rev/min] (Fig. 6), variation of hydraulic power generated by the pump  $P_h$  [W] (Fig. 7), variation of power absorbed by the electric motor  $P_a$  [W] (Fig. 8), all depending on pump discharge pressure  $p$  [bar].

## 2. Numerical simulations on energy recovery in endurance tests on positive displacement machines

### 2.1. Simulation model in AMESim

To study the dynamics of the energy recovery experimental demonstrative module the simulation model in AMESim [3] shown in Figure 9 has been used.

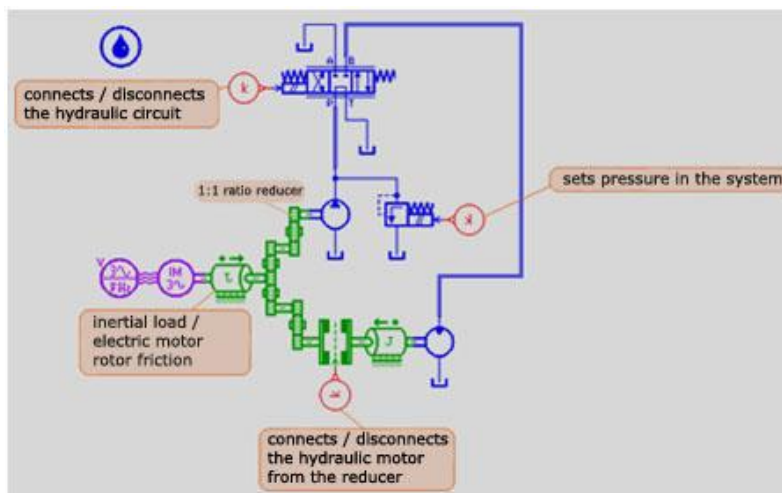


Fig. 9. Simulation model in AMESim

The AMESim model includes an inductive electric motor, to which a load has been introduced to simulate the inertial torque of the rotor and friction in the electric machine. To simulate system operation, in versions with and without energy recovery, a friction coupling has been introduced, which can be opened or closed, depending on the value of the excitation signal (0, and respectively 1).

For the hydraulic motor there is also the possibility of changing the load value, by changing the parameters of the inertial mass attached to its shaft.

Connecting and disconnecting the hydraulic circuit of the rotary positive displacement motor is carried out via the hydraulic directional control valve, and pressure in the system is set through the valve.

The two operating modes of the system are: with the hydraulic motor connected (with energy recovery) and with the hydraulic motor disconnected (without energy recovery).

In "connected" operating mode the signal "1" is sent to the coupling and the normally closed valve is set to the value of 30 bar.

In "disconnected" operating mode the excitation signal of the coupling is set to the value "0", to interrupt the mechanical connection between the electric motor and the hydraulic motor. The pressure in the system is then increased so that to the hydraulic motor shaft there is obtained the same rotational speed as for the "connected" hydraulic motor. Thus it is possible to compare the torques to the electric motor shaft, in the two operating modes, under the same loading conditions for the consuming positive displacement machines.

## 2.2. Results of numerical simulations

In the graph depicted by the Figure 10 one can notice that the torque of the electric motor drops after the hydraulic motor speed becomes equal to the electric motor speed (lag of 0.1 s).

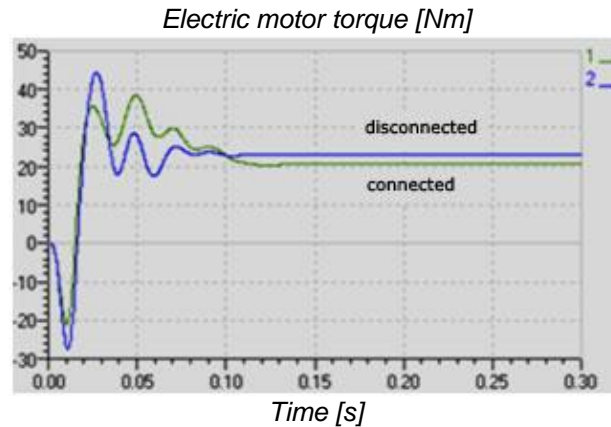


**Fig. 10.** Variation over time of electric motor (EM) torque, disconnected (1) / connected (2) from / to the hydraulic motor

In the graph depicted by the Figure 11 one can notice that the torque to the shaft attached to the reducer drops after the hydraulic motor speed becomes equal to the electric motor speed (lag of 0.1 s).

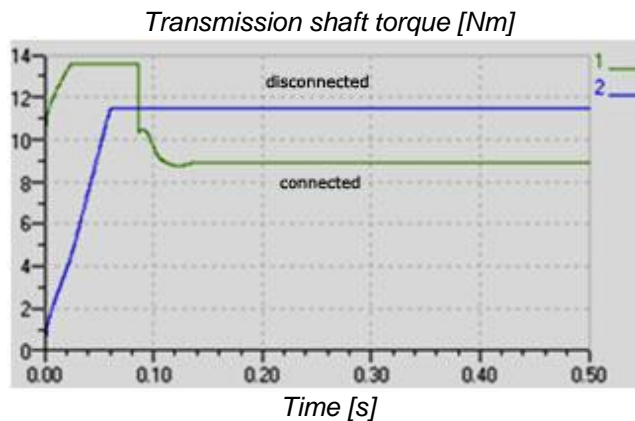


**Fig. 11.** Variation over time of torque to the reducer shaft; the EM disconnected (1) / connected (2) from / to the HM

In the graph depicted by the Figure 12 one can identify the time after which the hydraulic motor speed is equal to the electric motor speed (0.1 s - "connected", and respectively 0.4 s - "disconnected" from /to the electric motor).

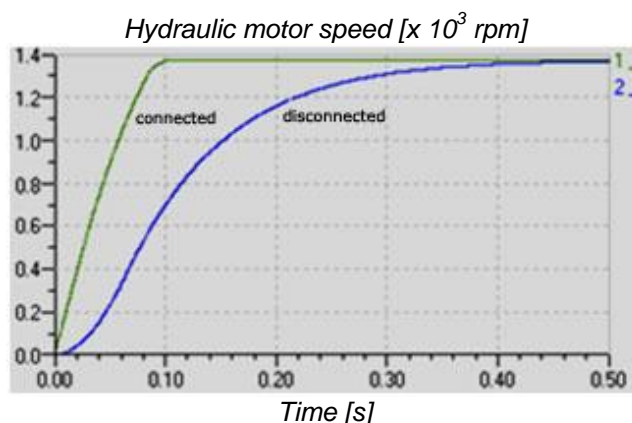


**Fig. 12.** Variation over time of hydraulic motor (HM) speed; disconnected (1) / connected (2) from / to the HM

In the Figure 13 one can notice the variation in flow through the pump, hydraulic motor and normally closed valve.

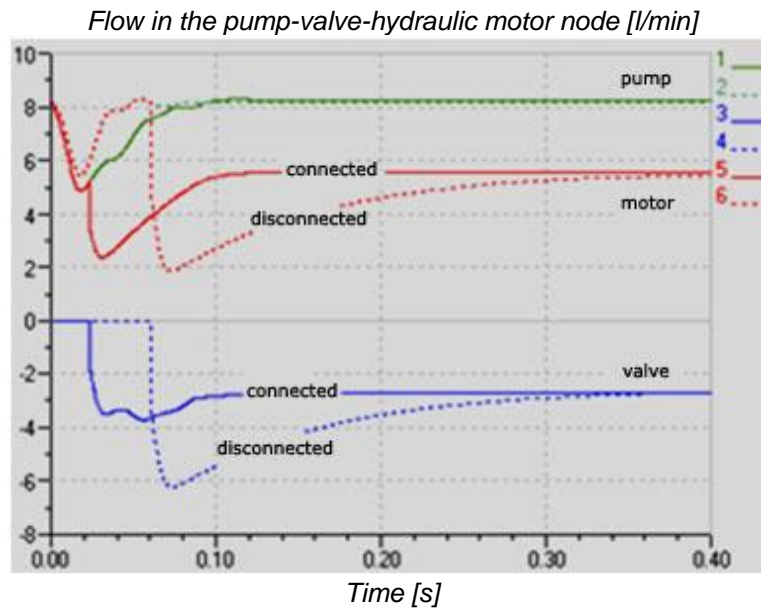


**Fig. 13.** Flow variation in the pump (1,2)–valve (3,4)-hydraulic motor (5,6) node

In the Figure 14 one can notice pressure variation in the pump-valve-directional control valve node.

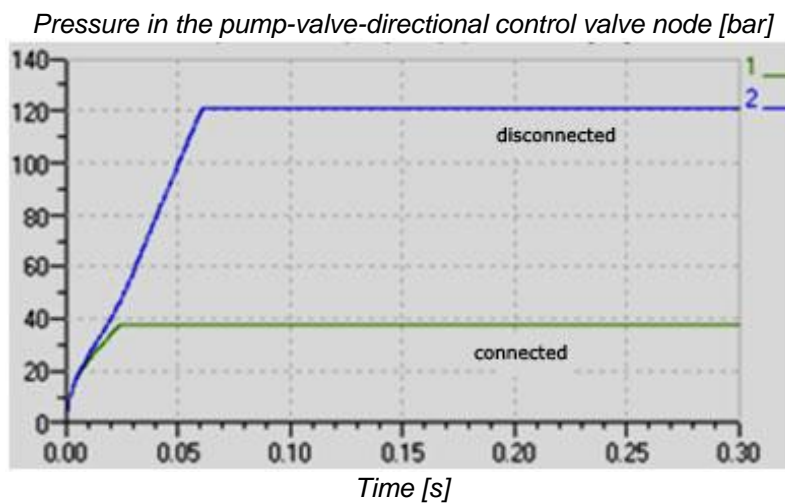


**Fig. 14.** Pressure variation in the pump-valve-directional control valve node; the EM disconnected (1) / connected (2) from / to the HM

## Conclusions

Experimental tests performed on the demonstrative module shown in Fig. 4 have demonstrated the efficiency of energy recovery, based on mechanical compensation of power losses, namely:

- powering of the hydraulic motor coupled to the electric motor results in the doubling of the pressure produced by the demonstrative stand, for the same current absorbed by the electric motor. For instance, for  $I=2A$ , there results  $p=36 \text{ bar}$ , when the hydraulic motor is not powered by the pump, and respectively  $p=80 \text{ bar}$ , when the hydraulic motor is powered by the pump (Fig. 5);

- powering of the hydraulic motor coupled to the electric motor results in the doubling of the pressure produced by the demonstrative stand, for the same speed of the electric motor. For instance, for  $n=1300 \text{ rpm}$ , there results  $p=20 \text{ bar}$ , when the hydraulic motor is not powered by the pump, and respectively  $p=40 \text{ bar}$ , when the hydraulic motor is powered by the pump (Fig. 6);
- pump maximum hydraulic power and maximum pressure produced by the stand are:  $P_h=480 \text{ W}$ ;  $p=48 \text{ bar}$ , when the hydraulic motor is not powered, and respectively  $P_h=1040 \text{ W}$ ;  $p=90 \text{ bar}$ , when the hydraulic motor is powered (Fig. 7);
- powering of the hydraulic motor coupled to the electric motor results in the doubling of the pressure produced by the demonstrative stand, for the same power absorbed by the electric motor. For instance, for  $P_a=800 \text{ W}$ , there results  $p=25 \text{ bar}$ , when the hydraulic motor is not powered by the pump, and respectively  $p=60 \text{ bar}$ ,  $p$  when the hydraulic motor is powered by the pump (Fig. 8).

Numerical simulations performed on the AMESim model shown in Fig. 9 have demonstrated the dynamic performance of the energy recovery system based on mechanical compensation of power losses, namely:

- connecting of the hydraulic motor to the shaft of the reducer (with 1:1 transmission ratio) results in lower torque developed by the electric motor, following a lag of 0.1 s (Fig. 10);
- connecting of the hydraulic motor to the shaft of the reducer results in lower torque developed by the electric motor, after the moment when the speeds of the two motors become equal, with a lag of 0.1s (Fig. 11);
- the time in which the hydraulic motor speed equals the electric motor speed is of 0.1 s, when the hydraulic motor is connected to the electric motor, and respectively 0.4 s, when the hydraulic motor is disconnected from the electric motor (Fig. 12);
- after 0.3 s from connecting the hydraulic motor to the electric motor pump flow is equal to the sum of flow through the hydraulic motor and flow through the pressure control valve (Fig. 13);
- speed achieved by the hydraulic motor at a pressure of 40 bar when it is mechanically connected to the electric motor is equal to hydraulic motor speed at a pressure of 120 bar when it is mechanically disconnected from the electric motor (Fig. 14).

All the conclusions listed, demonstrating the benefits of energy recovery by mechanical compensation for power losses, have applicability to the endurance stands of rotary and linear positive displacement machines (pumps, hydraulic motors, hydraulic cylinders).

### Acknowledgments

This paper has been developed in INOE 2000-IHP, with the financial support of the Executive Agency for Higher Education, Research, Development and Innovation Funding (UEFISCDI), under PN III, Programme 2- Increasing the competitiveness of the Romanian economy through research, development and innovation, Subprogramme 2.1- Competitiveness through Research, Development and Innovation - Innovation Cheques, project title: "Power recirculation stand for testing hydraulic cylinders", Financial Agreement no. 50 CI/2017.

### References

- [1] N. Vasiliu, D. Vasiliu, "Fluid Power Systems" („Acționări hidraulice și pneumatice”), Vol. I, Technical Publishing House, Bucharest, 2005, ISBN: 973-31-2248-3;
- [2] T.C. Popescu, P. Drumea, D.D. Ion Guta, I. Balan, "Power recirculation stand for endurance tests on hydraulic cylinders" ("Stand cu recirculare de putere pentru anduranța cilindrilor hidraulici”), Patent No. 127042/30.09.2016;
- [3] AMESim Software Suit.